

**Morphological and molecular characterization of the small armoured
dinoflagellate *Heterocapsa minima* (Peridiniales, Dinophyceae).**

Rafael Salas* ¹, Urban Tillmann², Siobhan Kavanagh³

¹Marine Institute, Renville, Oranmore, Co.Galway, Ireland

²Alfred Wegener Institute for Polar and Marine Research, Am Handelshafen 12, D-
27570 Bremerhaven, Germany.

³National University of Ireland, Galway, Ireland

***Corresponding author; Tel. 00 353 91 387241, e-mail: rafael.salas@marine.ie**

Abstract

The dinophycean genus *Heterocapsa* is of considerable interest, as it contains a number of bloom-forming and/or harmful species. Fine structure of organic body scales is regarded as the most important morphological feature for species determination but currently is unknown for the species *H. minima* described by Pomroy 25 years ago. Availability of a culture of *H. minima* collected in the Southwest of Ireland allowed us to provide important information for this species, including cell size, cell organelle location, thecal plate pattern, body scale fine structure, and molecular phylogeny. Light microscopy revealed the presence of one reticulate chloroplast, an elongated centrally located nucleus, and the presence of one pyrenoid surrounded by a starch sheath. Scanning electron microscopy (SEM) of the thecal plate pattern indicated that Pomroy erroneously designated the narrow first cingular plate as a sulcal plate. In addition, SEM revealed as yet unreported details of the apical pore complex and uncommon ornamentations of hypothecal plates. Organic body scales of *H. minima* were about 400 nm in size, roundish, with a small central hole and one central, six peripheral and three radiating spines. They differ from other body scales described within this genus allowing for positive identification of *H. minima*. *H. minima* shares gross cell morphological features (hyposome smaller than episome, elongated nucleus in the middle of the cell, one pyrenoid located in the episome on its left side) with *H. arctica* (both subspecies *H. arctica* subsp. *arctica* and *H. arctica* subsp. *frigida*), *H. lanceolata* and *H. rotundata*. These relationships are reflected in the phylogenetic trees based on LSU and ITS rDNA sequence data, which identified *H. arctica* (both subspecies), *H. rotundata* and *H. lanceolata* as close relatives of *H. minima*.

Keywords: Body scales, Dinophyceae, *Heterocapsa minima*, morphology, phylogeny, taxonomy.

Introduction

The dinophycean genus *Heterocapsa* is one of many genera erected by Stein (1883). Initially defined for species without visible plates on the hypotheca, after a taxonomic history thoroughly summarized by Iwataki (2008), the genus now comprises thecate peridinean species mainly characterized by the presence of organic three-dimensional body scales. These scales, which were first described for the type species *Heterocapsa triquetra* (Ehrenberg) Stein by Pennick & Clarke (1977), are unique to the genus and have species-specific fine structure, which makes them the most important morphological feature used in species designation (Iwataki *et al.*, 2004).

The thecal plate pattern of the genus is currently defined as (Kofoidian notation): Po, X, 5', 3a, 7'', 6C, 5S, 5''', 0-1p, 2'''''. However, a different plate pattern was described (Lindemann, 1924; Balech, 1988) for the type, *H. triquetra*, based on *Glenodinium triquetrum* Ehrenberg (1840), which needs to be clarified. Species currently assigned to *Heterocapsa* have repeatedly been shown to form a monophyletic group (Yoshida *et al.*, 2003; Zhang *et al.*, 2007; Stern *et al.*, 2012) that is poorly resolved relative to other Peridinales groups and sometimes occupies a basal position (Saldarriaga *et al.*, 2004; Zhang *et al.*, 2007). Furthermore, species of *Heterocapsa* have been shown to divide by desmoschisis (Morrill & Loeblich, 1984) which is quite uncommon within the Peridinales (Tillmann & Elbrächter, 2013), the sulcal plates are somewhat atypical (Saldarriaga *et al.*, 2004) and the earliest fossils of the family are recorded prior to the radiation of other Peridiniphyceidae (Fensome *et al.*, 1993).

In addition to these peculiarities, the genus is of ecological importance as a number of species, including *H. triquetra* and *H. rotundata* (Lohmann) Hansen, seem to be cosmopolitan and are known to form dense coastal blooms (Lindholm & Nummelin, 1999; Throndsen *et al.*, 2007). Most importantly, *H. circularisquama* Horiguchi is a harmful species (Nagai *et al.*, 1996) which caused large scale bivalve mortalities in Japan in 1992 (Matsuyama *et al.*, 1997) and is a serious threat to the Japanese and Hong Kong mussel industry. The discovery of this species and the obvious need to discriminate it correctly and without ambiguity from other co-occurring *Heterocapsa* species have driven many studies on the genus *Heterocapsa* in Japan in the last fifteen years (Horiguchi, 1995; Horiguchi, 1997; Matsuyama *et al.*, 1997; Matsuyama, 1999; Iwataki *et al.*, 2002a, 2002b; 2003, 2004, 2009; Tamura *et al.*, 2005; Iwataki 2008).

Almost all of the 17 currently accepted species are well described with respect to detailed morphology of the cells and of the body scales, based on culture material, and, in part, in terms of their rRNA sequence data. For two species, *H. pacifica* Kofoid and *H. minima* Pomroy, however, such detailed data are still missing.

Heterocapsa minima was described by Pomroy (1989) based on samples collected in the Celtic Sea in 1982–1983 at station CS2 (50° 30' N; 07° 00' W) northwest of the Scilly Isles, southwest England. Since then, it has been reported rarely. Hansen (1995) presented a body scale of a Danish isolate designated as *H. cf. minima*, but this culture was lost before being further characterized and unambiguously identified. Although Pomroy (1989) presented a detailed analysis of the thecal plate pattern of *H. minima* using electron microscopy, important morphological details of the cells, including presence or absence of a pyrenoid with a visible starch shield, are less clear. Most importantly, structural details of the body scales, regarded as the most

important morphological criterion for species designation (Iwataki *et al.*, 2004) are not defined for *H. minima* and there are no sequence data.

The aim of our study was to close this knowledge gap. Based on a culture of *H. minima* established from coastal waters in southwest Ireland, we present a detailed study of the cellular morphology, thecal plate tabulation and body scale ultrastructure of the species, and provide a phylogenetic analyses of LSU rRNA and ITS sequences.

Materials and Methods

Sample collection, isolation and culture of Heterocapsa minima

The culture of an Irish strain of *Heterocapsa minima* provisionally designated as JK2 was established from a water sample collected in southwest Ireland, at Gearhies pier, Bantry Bay (latitude: 51° 39' 4.7'' N, longitude: 9° 35' 11'' W) in September 2009.

Dinoflagellates were isolated as single cells by micropipette in 96 cell tissue culture plates (Corning, New York, USA). The isolates were kept in F/2 medium without silica (Guillard & Ryther, 1962; Guillard, 1975) made up with enriched sterile filtered seawater from the site and kept at 18° C, 12:12 light:dark cycle with irradiance 150 $\mu\text{mol photon m}^{-2} \text{s}^{-1}$ measured using an Iso-tech ILM 350 light meter (ISO-tech, Merseyside, UK). After successful isolation, the unialgal and clonal culture of JK2 was transferred to 25 x 150 mm borosilicate culture tubes (Fisherbrand™, Loughborough, UK) containing 35 ml of F/2 media and incubated in the conditions described.

Microscopy

Light microscopy (LM)

Observation of live or fixed (formalin: 1% final concentration; or neutral Lugol's-fixed: 1% final concentration) cells was carried out using an inverted microscope (Axiovert 200M, Zeiss, Germany) and a compound microscope (Axiovert 2, Zeiss, Germany) equipped with epifluorescence and differential interference contrast optics. Light microscopical examination of the thecal plate was performed on formalin-fixed cells (1% final concentration) stained with Calcofluor White (Fritz & Triemer, 1985). The shape and location of the nucleus was determined after staining formalin-fixed cells for 10 min with 4'-6-diamidino-2-phenylindole (DAPI, $0.1 \mu\text{g ml}^{-1}$ final concentration). Photographs were taken with a digital camera (AxioCam MRc5, Zeiss, Germany).

Cell length and width were measured at 1000 x magnification using Zeiss Axiovision software (Zeiss, Germany) on freshly fixed cells (formalin final concentration 1%) of a healthy and growing culture (based on stereomicroscopic inspection of the live culture).

Scanning electron microscopy (SEM)

For SEM, cells were collected by centrifugation (Eppendorf 5810R, Hamburg, Germany, 3220 g for 10 min) of 2–15 ml culture depending on cell density. The supernatant was removed and the cell pellet re-suspended in 60% ethanol in a 2 ml microtube for 1 h at 4° C to strip off the outer cell membrane. Subsequently, cells were pelleted by centrifugation (5 min, 16,000 g, Eppendorf centrifuge 5415 R) and re-suspended in a 60:40 mixture of deionized water and seawater for 30 min at 4° C. After centrifugation and removal of the diluted seawater supernatant, cells were fixed with

formalin (2% final concentration in a 60:40 mixture of deionized water and seawater) and stored at 4° C for 3 h. Cells were then collected on polycarbonate filters (Millipore, 25mm Ø, 3 µm pore-size) in a filter funnel where all subsequent washing and dehydration steps were carried out. Eight washings (2 ml MilliQ-deionized water each) were followed by a dehydration series in ethanol (30, 50, 70, 80, 95, 100%; 10 min each). Filters were dehydrated with hexamethyldisilazane (HMDS), initially 1:1 HMDS:EtOH followed by 2 x 100% HMDS, and stored under gentle vacuum in a desiccator. Finally, filters were mounted on stubs, sputtercoated (Emscope SC500, Ashford, UK) with gold-palladium and viewed under a scanning electron microscope (FEI Quanta FEG 200, Eindhoven, Netherlands). Some SEM micrographs were presented on a black background using Adobe Photoshop 6.0 (Adobe Systems, San Jose, USA).

Transmission electron microscopy

Whole mount preparations for the investigation of body scales were prepared in Formvar/carbon coated 75 mesh grid (Agar Scientific, Essex, UK) following the protocol by Hansen (1995). A drop of Poly-L-Lysine (Sigma Aldrich, Wicklow, Ireland) was used to aid the adhesion of cell tissue to the grid. A drop of 2% solution Osmium tetroxide (Sigma Aldrich, Wicklow, Ireland) was poured onto the grid and the sample was fixed for 20 min. After fixation the grid was rinsed with de-ionized water for 10 minutes, dried and stained with 2% aqueous Uranyl acetate (Sigma Aldrich, Wicklow, Ireland) for 2 min and rinsed. The transmission electron microscope used was a Hitachi 7500 operated at 75kV.

Molecular analyses

DNA extraction and PCR amplification

DNA was extracted from 10 ml culture of strain JK2 centrifuged (Eppendorf 5430, Hamburg, Germany) at 18000 rpm using the QIAGEN DNeasy plant mini kit (mini protocol without TissueRuptor/TissueLyser steps) under manufacturer conditions. DNA was eluted in 100 μ l AE buffer. Five μ l of the resulting DNA extract was run on a 1% agarose gel containing 10 μ g ml⁻¹ ethidium bromide using standard conditions to confirm the presence of high molecular weight DNA.

Primers (TIB MolBiol, Berlin) for PCR amplification of *H. minima* ITS and LSU regions were the primer pair ITS1 & ITS4 (D'Onofrio *et al.*, 1999) to target the entire ITS1, 5.8S and ITS2 regions and the primer pair DIR & D2C (Edwardsen *et al.*, 2003) to target the LSU D1-D2 region. PCRs were performed using the LightCycler® FastStart DNA Master HybProbe kit (Roche) in a total reaction volume of 20 μ l. A 1 x reaction mix contained 2 μ l LightCycler® FastStart enzyme reaction mix, 2 μ l MgCl₂ Stock Solution (25 mM concentration), 13 μ l PCR grade H₂O, 0.5 μ l primers (final concentration 12.5 pmol μ l⁻¹) and 2 μ l DNA extract template.

Amplification was carried out on the LightCycler 480™ under the following conditions: 95 °C for 10 min, followed by 45 cycles of 95 °C for 10 s, 50 °C for 15 s and 72 °C for 10 s. Amplicons were analysed by electrophoresis on 1% agarose as previously described.

The same protocol and primers were used to sequence the *H. rotundata* strain K-0483 from the Scandinavian culture collection of Algae and Protozoa (SCCAP).

Sequencing and phylogenetic analysis

PCR products of *H. minima* and *H. rotundata* strain K-0483 were sent for sequencing to Sequiserve Germany. Consensus reads were performed for both the ITS and LSU sequences. Closely related *Heterocapsa* ITS and LSU region sequences were identified using the BLAST tool at the NCBI website and were downloaded in FASTA format. Multiple sequence alignments using the LSU and ITS region sequences were generated using the MUSCLE program (Edgar, 2004) implemented in MEGA v5.2.1. (Tamura *et al.*, 2011). The alignments were edited manually so that only positions of unimpeachable homology were used for further phylogenetic analysis. Representatives from the *Prorocentrum* genus were included in the alignments as outgroup sequences. Phylogenetic trees were generated using MEGA v5.2.1. For each alignment, the model of DNA evolution that was the best fit to the data was found based on the lowest Bayesian Information Criterion (BIC) score (K2 +G for the LSU and K2+G for the ITS alignments respectively). Maximum Likelihood (ML), Neighbor-joining and Maximum Parsimony were used to generate trees. Bootstrap analysis (1000 replicates and 10 random addition sequences) was performed on all resulting trees. Only the ML trees are presented in this study. Uncorrected genetic distances (P-distance; Litaker *et al.*, 2007) were calculated from pairwise sequence comparisons and determined using MEGA.

Results

Cellular morphology

Cells of *H. minima* strain JK2 are ellipsoidal, elongate, and slightly dorso-ventrally compressed (Figs 1–7). When measured from freshly formalin-fixed cells using LM, they range in size from 10.0–13.0 μm in length (mean $11.8 \pm 0.6 \mu\text{m}$, $n = 106$) and 6.9–

9.1 μm in width (mean $8.1 \pm 0.5 \mu\text{m}$; $n = 106$). Cell size measurements made during SEM analysis (length range: 7.3–12.9 μm , mean $10.2 \pm 1.1 \mu\text{m}$, $n = 104$, epitheca width range: 5.7–9.0 μm , mean $7.1 \pm 0.6 \mu\text{m}$, $n = 68$) indicate a significantly reduced mean size of fixed and dehydrated cells (compare Figs 21, 22). The epitheca is roughly double the length of the small hypotheca. The maximum width of the hypotheca is slightly reduced accounting for $91 \pm 3\%$ (mean of 100 LM measurements) or $92 \pm 3\%$ (mean of 66 SEM measurements) of the maximum width of the epitheca. The cingulum is wide and accounts for 1/4 to 1/5 of the total cell length. The shape of the rounded to pointed episome is variable with the lateral outline ranging from convex to straight (Figs 1–6). The hyposome is rounded but could, at times, be slightly pointed (Fig. 1). A single large pyrenoid surrounded by a starch sheath is visible, consistently located in the episome (Fig. 3), and stained darkly with Lugol's iodine (Fig. 4). Calcofluor staining used to define the cell's orientation indicated that generally the pyrenoid is located laterally on the left side of the cell (compare Fig. 5 showing the pyrenoid and Fig. 6 showing the orientation (ventral view) of the same cell). A presumably single chloroplast of reticulate structure is present in the cell periphery extending into both the epi- and hyposome (Figs 7, 8). The nucleus is large and somewhat variable in shape ranging from oval to ellipsoid but is usually distinctly elongated and located in the middle of the cell, typically on the right side, with condensed chromosomes clearly visible (Figs 9–14). One nucleolus is visible at times (Fig. 13). A small red accumulation body may be present (Fig. 15). Cell division occurs in the motile stage by oblique binary fission (Fig. 16). Cells of *H. minima* generally move in a characteristic dinoflagellate swimming pattern of rotation and forward movement which sometimes, for unknown reasons, can change to a characteristic high speed back and forth motion in rapid succession or a

complete change of direction in a jumping action not dissimilar to *Azadinium* (Supplementary material).

Thecal plate morphology

The thecal plates of *H. minima* strain JK2 stained with Calcofluor White are shown in Figs 6, 17, 18. The exact plate pattern, as schematized in Figs 23–26, is more easily resolved by electron microscopy (Figs 19–21 & 27–40). The thecal plate configuration is: Po, cp, X, 5', 3a, 7'', 6C, 5s, 5''', 2'''''. It is similar to the original description by Pomroy (1989) but new details are described here.

In the epitheca there are 5 apical plates, 3 anterior intercalary plates with the central 2a plate being larger and seven sided and 7 precingular plates (Figs 27–31). The apical pore complex (APC) comprises an apical pore plate (Po) and a canal plate (X) and is presumably covered by a cover plate (cp). The Po plate has 6 symmetrically equidistant thecal pores arranged around the Po plate (Figs 31–33). Between the cp and the X plate there is an extra structure acting as a hinge or connection (Figs 32, 33). The X-plate is in contact with the first and fifth apical plate, displaced to the cell's right side and allows plate 1' to contact the pore plate.

The cingulum consists of 6 plates (Fig. 34). The first cingular plate (C1) is small and in contact with the anterior sulcal plate (Figs 34–36). In the sulcus we identified 5 plates: the largest plate extending into the epitheca, a right sulcal plate (rs) as a right termination of the cingulum, an anterior and a posterior left sulcal plate (las and lps) and a large posterior sulcal plate (ps) (Figs 35, 36). A few scales have been observed in our SEM preparations attached to the plate surface (Figs 37, 38). Among the hypothecal plates (5 postcingular and 2 antapical plates), a number of plates can be distinctly

ornamented with surface reticulations (Figs 39, 40), a feature never found on epithelial plates.

A number of trichocyst pores were also present on the cell surface; very often the location of these pores was difficult to detect because plates were masked by attached material. However, when visible these pores with an inner diameter of $0.17 \pm 0.1 \mu\text{m}$ ($n = 20$) consistently formed rows on both pre- and postcingular plates towards the cingulum with about 3 to 6 pores per plate. Likewise, rows of pores were detected on both posterior and anterior margins of all cingular plates except for C1. Other epithelial plates may have a few pores in a more scattered arrangement. One (or rarely two) pores were detected on the right lateral side of the posterior sulcal plate (Fig. 37). The antapical plates were characterized by rows of pores (4-6 on plate 2''''; 2-4 pores on plate 1''''') which most typically were accentuated by ornamentation (Figs 39, 40).

Body scale morphology

The diameter of *H. minima* body scales is $400 \pm 40 \text{ nm}$ ($n = 30$). The outline of the basal plate is triangular to round (Figs 41–44). The body scale structure of *H. minima*, when analysed using the morphological descriptors from Iwataki *et al.* (2004), is as follows: There are no spines on the basal plate but there is a small central hole (Figs 42, 43); the tri-dimensional structure consists of one central and 6 peripheral uprights or spines and 3 ridges which radiate and divide into 6 on the basal plate. Also, it has 3 radiating spines raised from the basal plate which are supported by peripheral bars. The 6 peripheral bars go from the radiating spines across to the peripheral uprights (Figs 42–44).

Molecular genetic analysis

ML analysis of *Heterocapsa* LSU sequences placed *H. minima* (KF031312) in a strongly supported clade with two accessions of *H. rotundata* (KF240778 and AF260400) and *H. arctica* subsp. *arctica* Horiguchi (AY571372) (Fig. 45). A third sequence (EU165312) designated as *H. rotundata*, however, was placed in a clade comprising *H. pygmaea* Loeblich III, Schmidt & Sherley (FJ939577) and an undetermined *Heterocapsa* species (EU165271).

A ML tree based on ITS sequences (Fig. 46) grouped *H. minima* (KF031311) with *Heterocapsa* sp. JD-2012 (JX661019, a cell called “Vil-39 holobiont” isolated from the radiolarian *Acanthochiasma* sp. by Decelle *et al.* (2012b)). *H. arctica* sequences (*H. arctica* subsp. *arctica*: JQ972677, AB084095; *H. arctica* subsp. *frigida* Rintala & G.Hällfors: HQ875058, HQ875057) were positioned as a closely related sister group with strong bootstrap support. *Heterocapsa rotundata* (KF240777) and *H. lanceolata* Iwataki & Fukuyo (AB084096) formed a less closely related clade, again supported by strong bootstrap values. ITS sequences of *H. minima* and Vil-39 exhibited 3 bp differences, resulting in an uncorrected p-distance value of 0.003, smaller than between *H. minima* and *H. arctica* (0.071 and 0.063 for *H. arctica* subsp. *arctica* JQ972677, AB084095; 0.063, and 0.066 for *H. arctica* subsp. *frigida* HQ875058, HQ875057, respectively) and between *H. minima* and *H. rotundata* (0.103).

Discussion

Within the genus *Heterocapsa* there are currently 17 accepted taxa; the 15 species listed by Iwataki (2008) updated with *H. huensis* Iwataki & Matsuoka and the newly described subspecies *H. arctica* subsp. *frigida* (Rintala *et al.*, 2010). Thecal plate pattern

and arrangement seem to be very similar for most of the *Heterocapsa* species and, in addition, to be variable within cultured strains (Hansen, 1995; Morrill & Loeblich, 1981), and are thus regarded as of limited value in species identification (Iwataki, 2008). Cell size and shape, in combination with shape and position of the nucleus and the number and location of pyrenoid(s), can be used to aid in species identification (Iwataki, 2008). Nevertheless, body scale fine structure is ultimately required for an unambiguous identification of most *Heterocapsa* species (Iwataki *et al.*, 2004). Scale structure had not been described for two *Heterocapsa* species (*H. pacifica* and *H. minima*) due to a lack of cultures or appropriate field samples. In particular, *H. minima* had not been unambiguously reported since its original description, although Hansen (1995) presented some preliminary observations (including a picture of a body scale) of a culture designated as *H. cf. minima*. However, this culture died before detailed investigations could be performed and since then, no other studies have focused on *H. minima*. We close the knowledge gap by describing cellular morphology, scale morphology, and molecular phylogeny of *H. minima*, which show that *H. minima* is a separate species distinctly different from all other described *Heterocapsa* species.

But firstly it is important to discuss why we think that our strain represents *H. minima*. Pomroy (1989) in his description of the species briefly mentioned the use of LM (inverted microscope for counting and fluorescence microscopy) but only provided SEM micrographs. Some of our cells in SEM preparations exactly resembled the holotype depicted by Pomroy (compare Fig. 22 with Pomroy's fig. 1) in terms of shape and general appearance. Moreover, similar characteristics include generally small size, the arrangement, size, and shape of thecal plates with a particularly narrow first cingular plate (although differently labelled by Pomroy, see discussion below), and a distinctly

smaller hypotheca compared to the epitheca. Finally, Pomroy described *H. minima* from the Celtic Sea, and even though our isolate originates from more inshore waters of the Irish coast there is convincing evidence that water of the latter is heavily influenced by and in connection with water of the Celtic Sea. Based on a decade-long programme on the Northwest European shelf, Hill *et al.* (2008), using satellite tracked drifting buoys, revealed that water mass around the Celtic Sea follows a highly organized thermohaline circulation. This circulation advects water through south and west St. George's Channel and directed south into the Celtic Sea and west along the Southern Irish coast (Brown *et al.*, 2003). Furthermore, there is evidence that this flow extends around the southwestern tip of Ireland (Raine & McMahon, 1998; Brown *et al.*, 2003; Hill *et al.*, 2008). Typical north-easterly winds in the region probably play an important role in the wind-driven advection of plankton into the bays of southwest Ireland (Raine *et al.*, 1990). We thus argue that both Pomroy's type locality (Celtic Sea) and the Irish southwest coastal waters are representative of the same water mass. This makes us confident that our strain JK2 indeed represents *H. minima*. However, there are a number of distinct differences between our strain and Pomroy's description

(1) The size range of *H. minima* given by Pomroy as $8.7 \pm 1.3 \mu\text{m}$ in length and $6.1 \pm 0.7 \mu\text{m}$ in width is distinctly smaller than our strain JK2 measured by LM on freshly formalin-fixed cells ($11.8 \pm 0.6 \mu\text{m}$ length, $8.1 \pm 0.5 \mu\text{m}$ width). Pomroy did not explicitly mention how he measured size but it seems quite probable that he measured cell dimensions from SEM micrographs. Without doubt, cells dehydrated during SEM preparation can significantly shrink, get wrinkled and can partly lose their shape (compare Figs 21, 22) causing a significant difference in mean size measurements using LM and SEM. In addition, size may vary depending on the culture conditions resulting

in larger size of cultured cells compared to field populations, although a slight long-term reduction in size of cultured *H. arctica* subsp. *arctica* indicates just the opposite (Rintala *et al.*, 2010). Generally, our LM measurements correspond with the cell of *H. cf. minima* depicted by Hansen (1995) (length: 11 μm , width: 8.6 μm) and we conclude that *H. minima* is not as extraordinarily small as in Pomroy's description and Iwataki's (2008) schematic drawings.

(2) Chloroplasts: Pomroy described *H. minima* as having numerous chloroplasts, parietally arranged. Our LM observations indicated one reticulate plastid in a parietal arrangement. A survey of chloroplast morphology of dinoflagellates indicates that larger species often possess numerous small and more globular plastids, whereas small species generally are characterized by one or very few large reticulate and parietally arranged chloroplasts (Schnepf & Elbrächter, 1999). Other species of *Heterocapsa*, which are all relatively small in size, have been described with one chloroplast (e.g. von Stosch, 1969; Rintala *et al.*, 2010). It is notoriously difficult using LM to show unequivocally whether there is one or more plastids. In epifluorescence microscopy, areas of bright fluorescence might be interpreted as separate chloroplasts, and conversely, seemingly connected and continuous plastid structures might in fact be separate plastids. Using TEM, Herman & Sweeney (1976) described chloroplast(s) of *H. illdefina* Morrill & Loeblich III as forming an interconnected network, but they still used the plural term "chloroplasts".

(3) Nucleus: We report the nucleus to be generally elongated and located in the middle of the cell on the right side. This seems to be in contradiction to Pomroy's description of a spherical nucleus posteriorly located. Size and shape of the dinophycean nucleus are known to vary among species, and also during different stages

of nuclear division (Dodge, 1963; Tillmann & Elbrächter, 2013). An elongated nucleus was not obviously restricted to certain stages of cell division but nuclear shape might depend on the cell orientation, causing an elongated nucleus to appear more oval (Fig. 14). In addition, nuclear shape might depend on other factors like fixation method or age of the samples.

(4) Pyrenoid: The presence of a pyrenoid, visible in LM due to its conspicuous starch sheath, was identified as one common character of the genus *Heterocapsa* (Iwataki, 2008). *Heterocapsa minima* also has one pyrenoid, which could be identified in all cells in the same position. However, because of the small size of the species, high magnification was needed to unambiguously identify the pyrenoids. Pomroy (1989) did not report the presence of a pyrenoid while using an inverted microscope and Lugol's-fixed samples for quantitative phytoplankton analysis. As Lugol's not only stains the starch shield of stalked pyrenoids (Fig. 6) but usually causes a dark brown staining of whole cells, it is probable that the pyrenoid was overlooked. In addition, Pomroy (1989) used fluorescence microscopy to determine chloroplast(s) and nuclear shape/location but epifluorescence cannot be used to detect pyrenoids.

In conclusion, we suggest that differences in terms of cell organelles (number of chloroplasts, shape and location of the nucleus, presence of a pyrenoid) between the original description of Pomroy (1989) and ours can be explained by observational differences and do not reflect true and significant differences in cell morphology. Nevertheless, more detailed microscopic observations on field populations and new cultures of *H. minima* are desirable.

In the context of Iwataki's comparative schema of other *Heterocapsa* species (Iwataki, 2008), *H. minima* obviously shares the characters hypotheca smaller than epitheca, elongated nucleus in the middle of the cell, one pyrenoid located in the middle of the cell on its left side with *H. arctica* (both subspecies), *H. lanceolata* and *H. rotundata*. *H. arctica* subsp. *arctica* and *H. lanceolata*, however, are generally larger in size (*H. arctica* subsp. *arctica*: 29.6 μm length, 11.6 μm width, Horiguchi 1997; *H. lanceolata*: 18.9 μm length, 11.6 μm width, Iwataki *et al.*, 2002a), although for *H. arctica* subsp. *frigida* there might be some overlap in size (12–19 μm length, 7.5–12 μm width (Rintala *et al.*, 2010) with *H. minima*. *Heterocapsa rotundata* is approximately the same size as *H. minima* but may have an even narrower hypotheca compared to the epitheca. However, both size and shape of *H. rotundata* has been reported to vary quite widely in natural samples (Rintala *et al.*, 2010). Sharing many characters with *H. rotundata*, a reliable and unequivocal identification of *H. minima* should thus include determination of the body scale structure (see below).

Thecal plates: In relation to the thecal plate morphology and arrangement of *H. minima*, there is one important difference in plate pattern diagnosis between Pomroy's (1989) interpretation and ours: The narrow and slightly oblique ventral plate, which we regard as the first cingular plate (C1), was designated by Pomroy as the left anterior sulcal plate "las". As a consequence, Pomroy's C1 is not in contact with the anterior sulcal plate, which would be a unique feature among species of *Heterocapsa*. This inconsistency was briefly discussed by Hansen (1995) and we now can confirm Hansen's interpretation that Pomroy overlooked one sulcal plate. Pomroy's "lps" plate (fig. 6, reproduced as Fig. 47) is actually two plates (lps and las) (Figs 35, 36. In continuation, with Pomroy's "las" plate being C1, his C1 would become C2 and so on,

meaning that Pomroy's cell would now have 7 cingular plates. However, we believe that there is no suture between his C1 and C2 (Fig. 36), therefore *H. minima*, like all other species of the genus, has 6 cingular plates (see Figs 28–30, 34). Our C2 plate starts roughly under the first pre-ingular plate suture (Figs 35, 36) and runs around to 2/3 of the second pre-ingular plate before the next suture (Figs 28, 36). In contrast, Pomroy's diagram (his fig. 7 (in our Fig.v47)) clearly shows C2 starting right under the second pre-ingular plate, but according to our SEM examinations there is no suture. Pomroy (1989) stated in his paper that “the delicate nature of the theca, coupled with the small size of some of the plates made their visualisation extremely difficult” and mentioned a general lack of contrast between plates and sutures, which we think is especially true for shrunken and wrinkled cells where folds easily can either mimic or obscure real sutures.

The characteristic ornamentation of hypothecal plates, visible in our Figs. 39, 40, has not been described previously for any species of *Heterocapsa*, but this could easily be because most other species descriptions were based exclusively on fluorescence microscopy-based plate pattern analysis. Therefore, SEM analysis of field populations are needed to clarify if these plate ornamentations are dependent on or modified by culture conditions.

Our detailed view of the APC of *H. minima* (Figs 32, 33) provides evidence for the presence of a cover plate neither indicated by Pomroy (1989) nor explicitly mentioned for other species of *Heterocapsa* (note that “cp” used here to abbreviate “cover plate” is occasionally used by others to designate a “canal plate”, another identifier of the X-plate). Coverage of the large apical pore by an extra plate is typical in many Peridinales. We also identified an extra plate-like structure acting like a hinge

joining the X-plate to the cover plate. The connection of X-plate and cover plate is strikingly similar to that found in the family Amphidomataceae (Tillmann *et al.*, 2009, 2012).

Body scales: In *Heterocapsa* this is the most important taxonomic criterion for identification to species level. A thorough analysis of all body scale information available (Iwataki *et al.*, 2004) revealed, as common characteristics, a tri-radiate structure of a basal plate and a tri-dimensional part made up of spines or uprights and horizontal bars (Fig. 44) and considered species-specific.

The body scales of *H. minima* cells have not been fully described before. Hansen (1995, fig. 4) showed a body scale from a *Heterocapsa cf. minima* culture but he was not able to establish whether the scale belonged to *H. minima*. Here we confirm that the body scale shown in Hansen (1995) belongs to *H. minima*, as the morphological characteristics between the scales of the Danish isolate and of *H. minima* JK2 (e.g the rounded triangular outline, three bifurcate ridges, a small central hole on the basal plate, and 6 peripheral spines; Hansen 1995, fig. 4) appear to be identical. The basal plate outline in *H. minima* is not clearly as circular as in *H. pygmaea* or *H. horiguchii* Iwataki, Takayama & Matsuoka, but not fully triangular as in *H. arctica* subsp. *arctica* or *H. rotundata*. We consider it to be circular in outline.

Scales of *H. minima*, with a mean diameter of 400 nm, are similar to *H. pygmaea*, *H. arctica* subsp. *frigida* and *H. circularisquama*. Scale size is not related to cell size in this genus – some of the smaller species have some of the largest body scales (as in *H. lanceolata* and *H. pygmaea*) and some of the largest species (as in *H. triquetra*,

H. pseudotriquetra Iwataki, G. Hansen & Fukuyo and *H. ovata* Iwataki & Fukuyo) have the smallest body scales.

The presence of a central hole, as identified here for *H. minima*, seems to be rare and has only been identified in *H. lanceolata* and *H. rotundata*. In *H. minima* the central hole is quite small and inconspicuous (Figs 42, 43) compared to the other two species. The presence of ridges on the basal plate is a character shared among all the species, the number of ridges ranging from 3 to 6 per species. In some species, this character is very clear with the ridges developing from the central upright and radiating along the surface of the basal plate to the outer diameter as in *H. arctica* (both subspecies), *H. circularisquama* or *H. lanceolata*. In *H. minima* it is not as clear as the 3 ridges radiate out halfway on the basal plate before each divides into 2, giving 6 ridges to the outer diameter of the body scale. The 3 radiating spines appear to emanate from the ridges. In *H. lanceolata*, *H. rotundata*, *H. huensis* or *H. illdefina* the radiating spines emanate from the central upright and they also appear between two ridges at an angle, whereas in *H. minima* the radiating spines are on top of the basal ridges before dividing to give the typical tri-lobed structure. We consider a ridge on the basal plate as the number of ridges commencing at the central upright, so *H. minima* has 3 ridges on the basal plate, although if we considered instead how many ridges develop on the surface of the basal plate to the outer diameter, then there would be 6. The three-dimensional construction of *H. minima* is not dissimilar to *H. circularisquama* with 6 peripheral uprights and 6 peripheral bars. Each bar joins a peripheral spine to a radiating spine as in *H. rotundata*, *H. lanceolata*, and *H. arctica* (both subspecies) but these have a different number of peripheral uprights.

Our study shows that the body scales of *H. minima* (Fig. 44), when compared to all the other described species (Table 1), are morphologically closer to *H. pygmaea*, *H. illdefina*, *H. huensis* and *H. rotundata*. However, peripheral spines, which are the most stable character because there are no changes between mature and immature body scales, are shared with *H. huensis*, *H. horiguchii*, *H. pygmaea*, *H. circularisquama* and *H. ovata*. *H. horiguchii*, *H. pygmaea*, *H. circularisquama* and *H. ovata* have 6 ridges on the basal plate compared to 3 in *H. minima* and *H. huensis* has no peripheral bars. Also, *H. pygmaea* has no peripheral uprights and *H. illdefina* and *H. rotundata* have 9 compared to 6 in *H. minima*. Therefore, based on body scale characters, *H. minima* can be differentiated to species level from all other *Heterocapsa* species.

Phylogenetic trees based on LSU and ITS rDNA sequence data are congruent in identifying the closest relatives of *H. minima* as *H. arctica* subsp. *arctica* and *H. rotundata*. *H. lanceolata* and *H. arctica* subsp. *frigida*, for which only ITS sequence data are available, are also closely related to *H. minima*. Generally, there are fewer LSU data available for the genus, with a large number of strains without a species designation and with a few examples of misidentified strains (e.g. *H. rotundata* EU161532).

ITS diverges more rapidly during speciation and has been successfully used to address phylogenetic questions and to resolve taxonomic ambiguities concerning dinoflagellates species (Yoshida *et al.*, 2003; Litaker *et al.*, 2007; Stern *et al.*, 2012). Probably because of its ability to resolve species of *Heterocapsa* (Yoshida *et al.*, 2003) there are many ITS sequences for the genus *Heterocapsa*, now including 14 of the described species. However, an ITS barcoding study has shown that sequence data of *Heterocapsa* strains have a particularly high level of mismatch to the given species

names (Stern *et al.*, 2012), corresponding to our “polyphyletic” placement of “*H. triquetra*” AF352364 within the *H. pygmaea* cluster and the placement by Stern *et al.* (2012) of FJ823556 (*H. niei* (Loeblich III) Morrill & Loeblich III under the ITS barcode identity “*H. pseudotriquetra*”

Comparing the sequence-based phylogenetic relation of *H. minima* to other species with the morphology-based categories discussed above, it is quite obvious that accordance in the size ratio of hypo- and epitheca as well as in location of cell organelles between *H. minima*, *H. arctica* (both subspecies), *H. rotundata* and *H. lanceolata* (see discussion above) is strikingly well reflected in the rRNA trees. On the contrary, parameters categorizing fine structural details of the body scales (see Table 1 and discussion above) seem to be less applicable to reflect synapomorphies of evolutionary related clades.

The most interesting finding is the high level of similarity of the ITS sequence data for *H. minima* and the isolate “Vil39-holobiont” (JX661019), a cell isolated from the acantharian *Acanthochiasma* sp. (Decelle *et al.*, 2012b, with 3 bp differences and an uncorrected p-distance of 0.003. In a general evaluation of ITS based genetic distance within and among dinoflagellate species, Litaker *et al.* (2007) found that for different species the uncorrected p-distance was always above 0.04, whereas within species p-distance could be as high as 0.021. More specifically, ITS-based genetic distance within species of *Heterocapsa* is in the range of 0 for *H. circularisquama*, 0.02–0.04 for *H. arctica* (considering both subspecies), and 0.02 for *H. horiguchii*. Excluding the most likely erroneous species designation of *H. triquetra* strain AF352364, genetic distance within *H. triquetra* is 0.000. On the other hand, uncorrected genetic distance of *H.*

minima to their closest related species is higher ($p = 0.063\text{--}0.103$), thereby clearly supporting our morphological evaluation that *H. minima* represents a separate species.

Thus, *H. minima* and the endosymbiotic *Heterocapsa* isolate (Vil39-holobiont), based on their almost identical ITS sequence data, should be considered as conspecific (Montresor *et al.*, 2003). However, identical ITS data do not necessarily imply conspecificity, as has been convincingly shown for *Scrippsiella hangoei* (Schiller) Larsen and *Peridinium aciculiferum* Lemmermann. These two taxa have identical ITS sequences (Gottschling *et al.*, 2005) but clearly are different in terms of phenotypes and habitat segregation, sufficient to regard them as two different species (Logares *et al.* 2007). Likewise, thresholds for divergence rates are probably problematic for endosymbionts. Formation of symbiotic relationships most likely provokes genetic isolation, as well as a suite of unique selection pressures depending on the environmental conditions within the host's habitat. For endosymbionts of the genus *Symbiodinium* there is evidence that such an isolation may give rise to new species with ITS genetic divergences < 0.04 (van Oppen *et al.*, 2001; LaJeunesse *et al.*, 2004).

Although isolate “Vil39-holobiont”, in spite of its ITS similarity to free living *H. minima*, might represent a distinct and specialized endosymbiotic species, also it is also possible that the cell isolated from the acantharia represented a cell of *H. minima* which had just been ingested and still had undigested DNA. Moreover, it is also conceivable that cells of free-living *H. minima* can be taken up by acantharian hosts, which then take control of the still-photosynthesizing microalgal cell; a situation perhaps better described as enslavement (Decelle *et al.*, 2012a) or controlled parasitism (Wooldridge, 2010) than mutually beneficial endosymbiosis. This would differ from other microalgae involved in symbiosis, which are specialized for a symbiotic lifestyle. These “true”

endosymbionts which require horizontal transmission in each generation, need to be able to thrive at least temporarily as a free-living stage when released and/or expelled by the hosts (Steele, 1977). The failure to establish a cell culture from the “*H. minima*” cell isolated from the acantharia (Decelle *et al.*, 2012b) might support the view that these ‘*H. minima*’ are no more than photosynthesizing entities no longer able to thrive on their own. On the other hand, viability as free living cells has been demonstrated for another *Heterocapsa* isolated from acantharia. ITS sequences of strain AC24-1 established from a single cell isolated from an acantharia (Decelle *et al.*, 2012b) indicated a close relationship, if not conspecificity, of this culture to *H. pygmaea* (FJ823558 & AB084094) or to AF352364 (designated as *H. triquetra*, but following Stern *et al.* (2012) this is probably a misidentification), with an uncorrected genetic distance of only 0.005 or 0.004, respectively.

In any case, a comparable scenario of genetic similarity in endosymbiotic and common free-living algal species was also considered likely for a number of acantharia harbouring cells which revealed DNA signatures identical to free-living species of *Phaeocystis* (Decelle *et al.*, 2012a). To conclude, our intriguing finding of almost identical ITS sequence data of free living *H. minima* and a cell isolated as “endosymbiont” from an acantharia calls for more detailed investigation.

Pomroy (1989) mentioned that *H. minima* is widely distributed in the continental shelf and deeper waters of the Celtic Sea and also in the Irish Sea. We isolated our *H. minima* strain from inshore southwestern Ireland, where the species co-occurs with other small armoured dinoflagellates such as *Azadinium* and *Amphidoma* (Salas *et al.*, 2011) and may be advected into bays by characteristic northeasterly winds. Water mass circulation on the Northwest European shelf would explain its wide distribution in the

Celtic Sea and around the Irish coast. These small armoured dinoflagellates appear to be a very common group in Irish waters. Monitoring data from the Irish National Biotoxins programme normally does not go beyond genus level in identifying small species and cannot even separate the genera *Heterocapsa*, *Azadinium* and *Amphidoma*.

Consequently, the spatial and temporal distribution of *H. minima* around the Irish coastline is not presently known. In any case, to date there have been no reports of direct harmful effects to shellfish or finfish caused by blooms of small species including *H. minima*. However, *H. minima* obviously co-occurs with species of *Azadinium*, the identified source organism of azaspiracid toxins (Tillmann *et al.*, 2009) in the water column. As these species are similar in terms of size and shape, in having a prominent pyrenoid and a somewhat similar swimming pattern, LM identification of azaspiracid-producing species in Irish coastal waters is seriously hindered.

Acknowledgments

This project (Grant-Aid Agreement No. PBA/AF/08/001(01)) was carried out under the *Sea Change* strategy with the support of the Marine Institute and the Marine Research Sub-Programme of the National Development Plan 2007–2013, co-financed under the European Regional Development Fund. We greatly acknowledge helpful comments and suggestion of Mitsunori Iwataki and Janne Rintala which improved the manuscript.

Supplementary information

The following supplementary material is accessible via the Supplementary Content tab on the article's online page at <http://dx.doi.org/10.1080/09670262.2014.956800> Video file showing *H. minima* swimming behaviour.

References

- BALECH, E. (1988). Los dinoflagellados del Atlántico sudoccidental. *Publicaciones Especiales Instituto Español de Oceanografía*, Madrid. 310 pp.
- BROWN, J., CARRILLO, L., FERNAND, L., HORSBURGH, K.J., HILL, A.E., YOUNG, E.F. & MEDLER, K.J. (2003). Observations of the physical structure and seasonal jet-like circulation of the Celtic Sea and St. George's Channel of the Irish Sea. *Continental Shelf Research*, **23**: 533–561.
- DECELLE, J., PROBERT, I., BITNERR, L., DESDEVISES, Y., COLIN, S., DE VARGAS, C., GALI, M., SIMO, R. & NOT, F. (2012a). An original mode of symbiosis in open ocean plankton. *Proceedings of the National Academy of Science*, **109**: 18000–18005.
- DECELLE, J., SIANO, R., PROBERT, I., POIRIER, C. & NOT, F. (2012b). Multiple microalgal partners in symbiosis with the acantharian *Acanthochiasma* sp. (Radiolaria). *Symbiosis*, **58**: 233–244.
- D'ONOFRIO, G., MARINO, D., BIANCO, L., BUSICO, E. & MONTRESOR, M. (1999). Toward an assessment on the taxonomy of dinoflagellates that produce calcareous cysts (Calciodinelloideae, Dinophyceae): a morphological and molecular approach. *Journal of Phycology*, **3**: 1063–1078.
- DODGE, J.D. (1963). The nucleus and nuclear division in the Dinophyceae. *Archiv für Protistenkunde*, **106**: 442–452.

EDGAR, R.C. (2004). MUSCLE: multiple sequence alignment with high accuracy and high throughput. *Nucleic Acids Research*, **32**:1792-1797.

EDVARDBSEN, B., SHALCHIAN-TABRIZI, K., JAKOBSEN, K.S., MEDLIN, L.K., DAHL, E., BRUBAK, S. & PAASCHE, E. (2003). Genetic variability and molecular phylogeny of *Dinophysis* species (Dinophyceae) from Norwegian waters inferred from single cell analyses of rDNA. *Journal of Phycology*, **39**: 395–408.

FENSOME, R.A., TAYLOR, F.J.R., NORRIS, G., SARJEANT, W.A.S., WHARTON, D.I. & WILLIAMS, G.L. (1993). A classification of living and fossil dinoflagellates. *Micropaleontology*, Special Publication **7**: 1–351.

FRITZ, L. AND TRIEMER, R. E. (1985). A rapid simple technique utilizing Calcofluor White M2R for the visualization of dinoflagellate thecal plates. *Journal of Phycology*, **21**: 662–664.

GOTTSCHLING, M., KEUPP, H., PLÖTNER, J., KNOP, R., WILLEMS, H. & KIRSCH, M. (2005). Phylogeny of calcareous dinoflagellates as inferred from ITS and ribosomal sequence data. *Molecular Phylogenetics and Evolution*, **36**: 444–455.

GUILLARD, R.R.L. (1975). Culture of phytoplankton for feeding marine invertebrates. In *Culture of Marine Invertebrate Animals* (Smith, W.L. & Chanley, M.H., editors), 26–60. Plenum Press, New York.

GUILLARD, R.R.L. & RYTHER, J.H. (1962). Studies of marine planktonic diatoms: I. *Cyclotella nana* Hustedt and *Detonula confervacea* Cleve. *Canadian Journal of Microbiology*, **8**: 229–239.

HANSEN, G. (1995). Analysis of the thecal plate pattern in the dinoflagellate *Heterocapsa rotundata* (Lohmann) comb. nov. (= *Katodinium rotundatum* (Lohmann) Loeblich). *Phycologia*, **34**: 166–170.

HERMAN, E.M. & SWEENEY, B.M. (1976). *Cachonina illdefina* sp. nov. (Dinophyceae): Chloroplast tubules and degeneration of the pyrenoid. *Journal of Phycology*, **12**: 198–205.

HILL, A.E., BROWN, J., FERNAND, L., HOLT, J., HORSBURGH, K.J., PROCTOR, R., RAINE, R. & TURRELL, W.R. (2008). Thermohaline circulation of shallow tidal seas. *Geophysical Research Letters*, **35**: L11605.

HORIGUCHI, T. (1995). *Heterocapsa circularisquama* sp. nov. (Peridiniales, Dinophyceae): a new marine dinoflagellate causing mass mortality of bivalves in Japan. *Phycological Research*, **43**: 129–136.

HORIGUCHI, T. (1997). *Heterocapsa arctica* sp. nov. (Peridiniales, Dinophyceae): a new marine dinoflagellate from the arctic. *Phycologia*, **36**: 488–491.

IWATAKI, M. (2008). Taxonomy and identification of the armoured dinoflagellate genus *Heterocapsa* (Peridinales, Dinophyceae). *Plankton and Benthos Research*, **3**: 135–142.

IWATAKI, M., TAKAYAMA, H., MATSUOKA, K., FUKUYO, Y. (2002a). *Heterocapsa lanceolata* sp. nov. and *Heterocapsa horiguchii* sp. nov. (Peridinales, Dinophyceae), two new marine dinoflagellates from coastal Japan. *Phycologia*, **41**: 470–479.

IWATAKI, M., WONG, M.W. & FUKUYO, Y. (2002b). New record of *Heterocapsa circularisquama* (Dinophyceae) from Hong Kong. *Fisheries Science*, **68**: 1161–1163.

IWATAKI, M., BOTES, L., SAWAGUCHI, T., SEKIGUCHI, K. & FUKUYO, Y. (2003). Cellular and body scale structure of *Heterocapsa ovata* sp. nov. and *Heterocapsa orientalis* sp. nov. (Peridinales, Dinophyceae). *Phycologia*, **42**: 629–637.

IWATAKI, M., HANSEN, G., SAWAGUCHI, T., HIROISHI, S. & FUKUYO, Y. (2004). Investigations of body scales in twelve *Heterocapsa* species (Peridinales, Dinophyceae), including a new species *H. pseudotriquetra* sp. nov. *Phycologia*, **43**: 394–403.

IWATAKI, M., KAWAMI, H., VAN NGUYEN, N., LUONG, Q.D., TON, T.P., FUKUYO, Y. & MATSUOKA, K. (2009). Cellular and body scale morphology of *Heterocapsa huensis* sp. nov. (Peridinales, Dinophyceae) found in Hue, Vietnam. *Phycological Research*, **57**: 87–93.

LAJEUNESSE, T.C., THORNHILL, D.J., COX, E.F., STANTON, F.G., FITT, W.K. & SCHMIDT, G.W. (2004). High diversity and host specificity observed among symbiotic dinoflagellates in reef communities from Hawaii. *Coral Reefs*, **23**: 596–603.

LINDEMANN, E. (1924). Der Bau der Hülle bei *Heterocapsa* und *Kryptoperidinium foliaceum* (Stein) n. nov. (zugleich eine vorl. Mitteilung). *Botanisches Archiv*, **5**: 114–120.

LINDHOLM, T. & NUMMELIN, C. (1999). Red tide of the dinoflagellate *Heterocapsa triquetra* (Dinophyta) in a ferry-mixed coastal inlet. *Hydrobiologia*, **393**: 245–251.

LITAKER, W., VANDERSEA, M.W., KIBLER, S.R., REECE, K.S., STOKES, N.A., LUTZONI, F.M., YONISH, B.A., WEST, M.A., BLACK, M.N.D. & TESTER, P.A. (2007). Recognizing dinoflagellate species using ITS rDNA Sequences. *Journal of Phycology*, **43**: 344–355.

LOGARES, R., RENGEFORS, K., KREMP, A., SHALCHIAN-TABRIZI, K., BOLTOVSKOY, A., TENGS, T., SHURLEFF, A. & KLAVENESS, D. (2007). Phenotypically different microalgal morphospecies with identical ribosomal DNA: A case of rapid adaptive evolution? *Microbial Ecology*, **53**: 549–561.

MATSUYAMA, Y. (1999). Harmful effect of dinoflagellate *Heterocapsa circularisquama* on shellfish aquaculture in Japan. *Japan Agricultural Research Quarterly*, **33**: 283–294.

- MATSUYAMA, Y., KIMURA, A., FUJII, H., TAKAYAMA, H. & UCHIDA, T. (1997). Occurrence of a *Heterocapsa circularisquama* red tide and subsequent damages to shellfish in western Hiroshima Bay, Seto Inland Sea, Japan in 1995. *Bulletin of the Nansei National Fisheries Research Institute*, **30**: 189–207.
- MONTRESOR, M., SGROSSO, S., PROCACCINI, G. & KOOISTRA, W.H.C.F. (2003). Intraspecific divergence in *Scrippsiella trochoidea* (Dinophyceae): evidence for cryptic species. *Phycologia*, **42**: 56–70.
- MORRILL, L.C. & LOEBLICH III, A.R. (1981). A survey for body scales in dinoflagellates and a revision of *Cachonina* and *Heterocapsa* (Pyrrhophyta). *Journal of Plankton Research*, **3**: 53–65.
- MORRILL, L.C. & LOEBLICH III, A.R. (1984). Cell division and reformation of the amphiesma in the pelliculate dinoflagellate, *Heterocapsa niei*. *Journal of the Marine Biological Association of the United Kingdom*, **64**: 939–953.
- NAGAI, K., MATSUYAMA, Y., UCHIDA, T., YAMAGUCHI, M., ISHIMURA, M., NISHIMURA, A., AKAMATSU, S. & HONJO, T. (1996). Toxicity and LD50 levels of the red tide dinoflagellate *Heterocapsa circularisquama* on juvenile pearl oysters. *Aquaculture*, **144**: 149–154.

PENNICK, N.C. & CLARKE, K.J. (1977). The occurrence of scales in the peridinian dinoflagellate *Heterocapsa triquetra* (Ehrenberg) Stein. *British Phycological Journal*, **12**: 63–66.

POMROY, A.J. (1989). Scanning electron microscopy of *Heterocapsa minima* sp. nov. (Dinophyceae) and its seasonal distribution in the Celtic Sea. *British Phycological Journal*, **24**: 131–135.

RAINE, R. & MCMAHON, T. (1998). Physical dynamics on the continental shelf off southwestern Ireland and their influence on coastal phytoplankton blooms. *Continental Shelf Research*, **18**: 883–914.

RAINE, R., O'MAHONEY, J., MCMAHON, T. & RODEN, C. (1990). Hydrography and phytoplankton of waters off southwest Ireland. *Estuarine Coastal and Shelf Sciences*, **30**: 579–596.

RINTALA, J-M., HÄLLFORS, H., HÄLLFORS, S., HÄLLFORS, G. MAJANEVA, M & BLOMSTER, J. (2010). *Heterocapsa arctica* subsp. *frigida* subsp. nov. (Peridiniales, Dinophyceae)-description of a new dinoflagellate and its occurrence in the Baltic Sea. *Journal of Phycology*, **46**: 751–762.

SALAS, R., TILLMANN, U., JOHN, U., KILCOYNE, J., BURSON, A., CANTWELL, C., HESS, P., JAUFFRAIS, T. & SILKE, J. (2011). The role of *Azadinium spinosum* (Dinophyceae) in the production of azaspiracid shellfish poisoning in mussels. *Harmful Algae*, **10**: 774–783.

SALDARRIAGA, F.J., TAYLOR, F.J.R., CAVALIER-SMITH, T., MENDEN-DEUER, S. & KEELING, P.J. (2004). Molecular data and the evolutionary history of dinoflagellates. *European Journal of Protistology*, **40**: 85–111.

SCHNEPF, E. & ELBRÄCHTER, M. (1999). Dinophyte chloroplasts and phylogeny - A review. *Grana*, **38**: 81–97.

STEELE, R.D. (1977). The significance of zooxanthella containing pellets extruded by sea-anemones. *Bulletin of Marine Science*, **27**: 591–594.

STEIN, F. (1883) Der Organismus der Infusionsthier. III. Abt. Der Organismus der Arthrodelen Flagellaten nach eigenen Forschungen in systematischer Reihenfolge bearbeitet. II. Hälfte. Einleitung und Erklärung der Abbildungen. W. Engelmann, Leipzig. pp.1-30

STERN, R.F., ANDERSEN, R.A., JAMESON, I., KÜPPER, F.C., COFFROTH, M-A., VAULOT, D., LE GAIL, F., VERON, B., BRAND, J.J., SKELTON, H., KASAI, F., LILY, E.L. & KEELING, P.J. (2012). Evaluating the Ribosomal Internal Transcribed Spacer (ITS) as a candidate dinoflagellate barcode marker. *PLoS ONE*, **7**: e42780.

VON STOSCH, H.A. (1969). Dinoflagellaten aus der Nordsee I. Über *Cachonina niei* Loeblich (1968), *Gonyaulax grindley* Reinecke (1967) und eine Methode zur

Darstellung von Peridiniidenpanzern. *Helgoländer Wissenschaftliche Meeresuntersuchungen*, **19**: 558–568.

TAMURA, M., IWATAKI, M. & HORIGUCHI, T. (2005). *Heterocapsa psammophila* sp. nov. (Peridinales, Dinophyceae), a new sand-dwelling marine dinoflagellate. *Phycological Research*, **53**: 303–311.

TAMURA, K., PETERSON, D., PETERSON, N., STECHER, G., NEI, M. & KUMAR, S. (2011). MEGA5: Molecular Evolutionary Genetics Analysis using Maximum Likelihood, Evolutionary Distance, and Maximum Parsimony Methods. *Molecular Biology and Evolution*, **28**: 2731–2739.

THRONDSSEN, J., HASLE, G.R. & TANGEN, K. (2007). *Phytoplankton of Norwegian Coastal Waters*. Almatel Forlag AS, Oslo, Norway, 343 pp

TILLMANN, U. & ELBRÄCHTER, M. (2013). Cell division in *Azadinium spinosum* (Dinophyceae). *Botanica Marina*, **56**: 399–408.

TILLMANN, U., ELBRÄCHTER, M., KROCK, B., JOHN, U. & CEMBELLA, A. (2009). *Azadinium spinosum* gen. et sp. nov. (Dinophyceae) identified as a primary producer of azaspiracid toxins. *European Journal of Phycology*, **44**: 63–79.

TILLMANN, U., SALAS, R., GOTTSCHLING, M., KROCK, B., O'DRISCOLL, D. & ELBRÄCHTER, M. (2012). *Amphidoma languida* sp. nov. (Dinophyceae) reveals a close relationship between *Amphidoma* and *Azadinium*. *Protist*, **163**: 701–719.

VAN OPPEN, M.J.H., PALSTRA, F.P., PIQUETA, M.T. & MILLER, D.J. (2001). Patterns of coral-dinoflagellate associations in *Acropora*: significance of local availability and physiology of *Symbiodinium* strains and host-symbiont selectivity. *Proceedings of the Royal Society of London of Biological Sciences*, **268**: 1759–1767.

WOOLDRIDGE, S.A. (2010). Is the coral-algae symbiosis really "mutually beneficial" for the partners? *Bioessays*, **32**: 615–625.

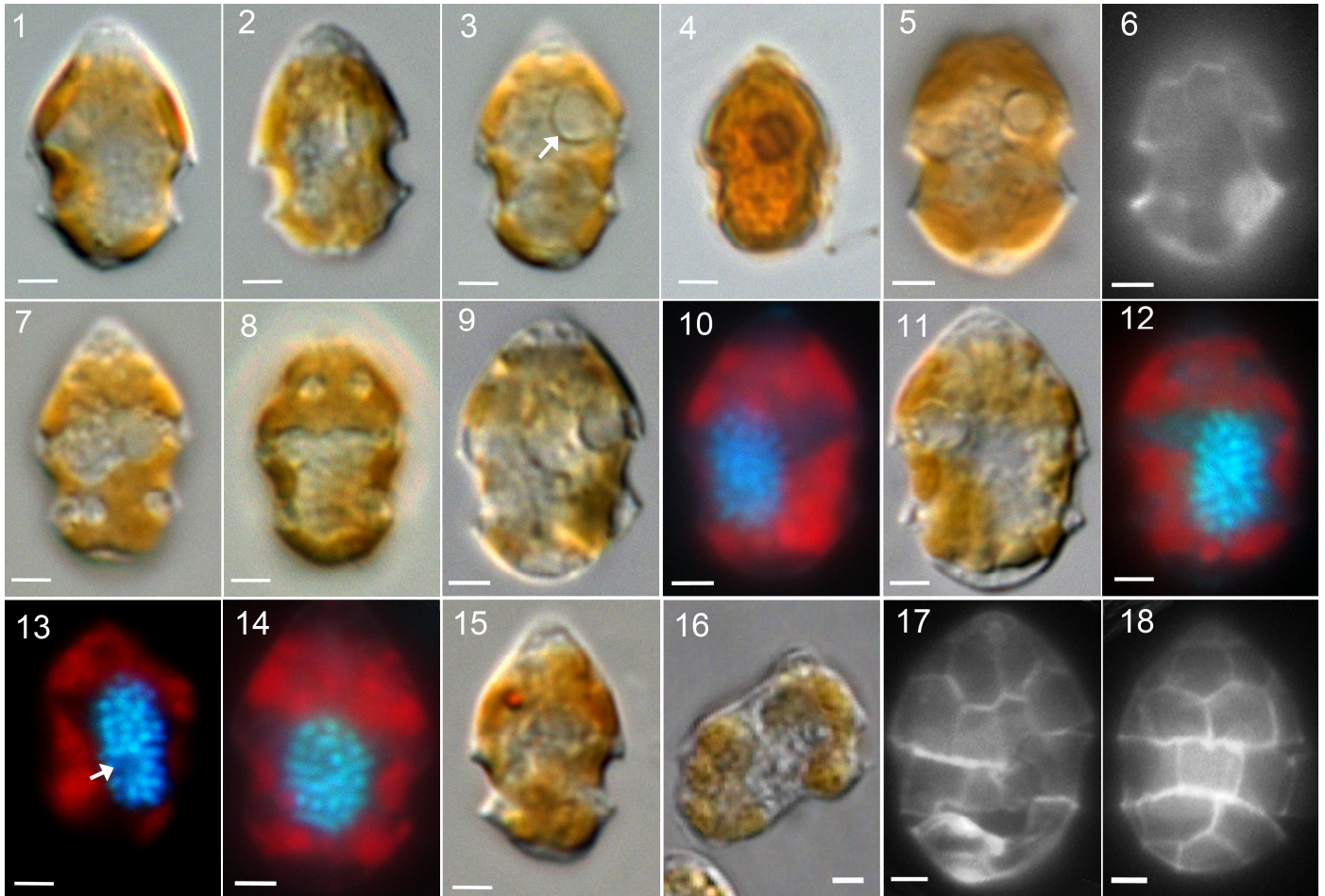
YOSHIDA, T., NAKAI, R., SETO, H., WANG, M-K., IWATAKI, M. & HIROISHI, S. (2003). Sequence analysis of 5.8S rDNA and the internal transcribed spacer region in dinoflagellate *Heterocapsa* species (Dinophyceae) and development of selective PCR primers for the bivalve killer *Heterocapsa circularisquama*. *Microbes and Environment*, **18** : 216–222.

ZHANG, H., BHATTACHARYA, D. & LIN, S. (2007). A three-gene dinoflagellate phylogeny suggests monophyly of prorocentrales and a basal position for *Amphidinium* and *Heterocapsa*. *Journal of Molecular Evolution*, **65**: 463–474.

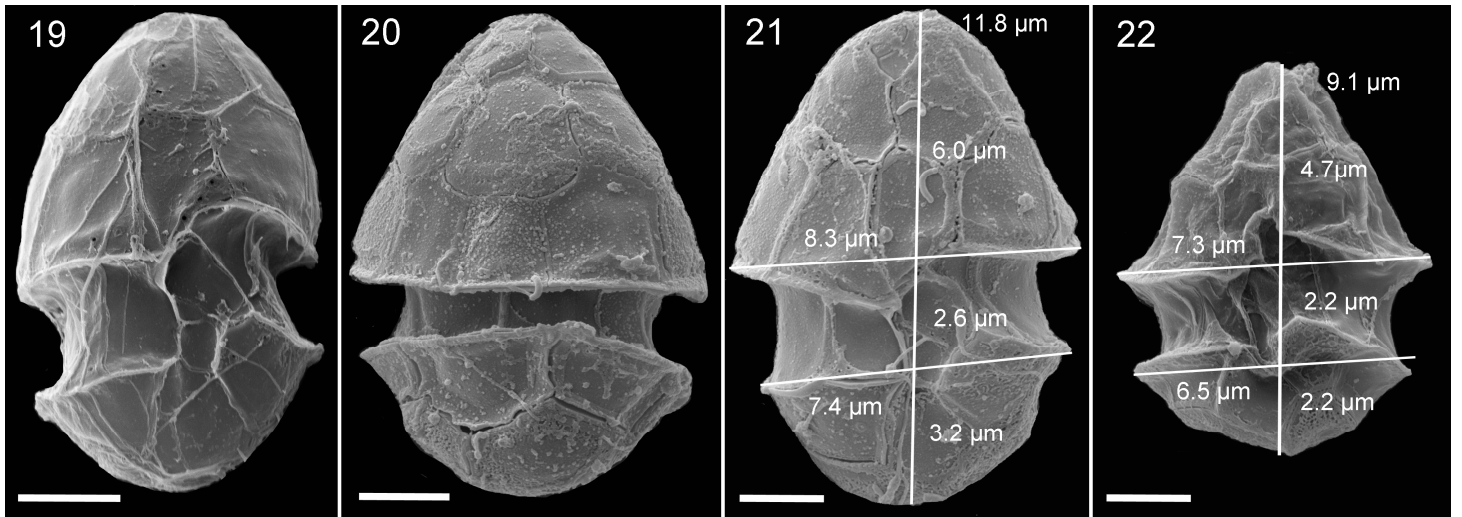
Table 1: Characters of body scale ultrastructure in *Heterocapsa* species taken from Iwataki *et al.* (2004) with the addition of *Heterocapsa minima*, *H. psammophila* (Tamura *et al.* 2005), *H. huensis* (Iwataki *et al.*, 2009) and *H. arctica* subsp. *frigida* (Rintala *et al.*, 2010) details.

Species	Diameter (nm)	Outline of basal plate	Ridges on basal plate	Central hole	Spines on basal plate	Central uprights (or spines)	Peripheral Uprights (or spines)	Peripheral bars	Strain
<i>H. arctica</i> subsp. <i>arctica</i> ^a	350	triangular	6	0	0	1	9	6	CCMP445
<i>H. arctica</i> subsp. <i>frigida</i> ^a	400	triangular	6	0	0	1	9	0	755
<i>H. circularisquama</i> ^a	400	circular	6	0	0	1	6	6	HCHS95
<i>H. horiguchii</i>	310	circular	6	0	0	1	6	0	FK6-D47
<i>H. huensis</i>	550	triangular	6	0	0	1	9	6	
<i>H. illdefina</i>	430	triangular	6	0	0	1	9	0	CCMP446
<i>H. lanceolata</i>	500	hexagonal	3	1	0	1	9	12	TK6-D57
<i>H. minima</i>	400	circular	3	1	0	1	6	6	JK2
<i>H. niei</i> ^a	300	triangular	3	0	3	1	15	18	NIES 420
<i>H. orientalis</i>	300	triangular	6	0	0	1	9	12	D-127-C-3
<i>H. ovata</i>	220	triangular	6	0	0	1	6	9	KZHt-1
<i>H. psammophila</i>	230	triangular	6	1	0	1	9	12	
<i>H. pygmaea</i>	400	circular	6	0	0	1	6	0	CCMP1490
<i>H. rotundata</i>	350	triangular	6	1	0	1	9	6	TK12-D44
<i>H. triquetra</i>	250	triangular	6	0	0	1	9	12	TK12-D40

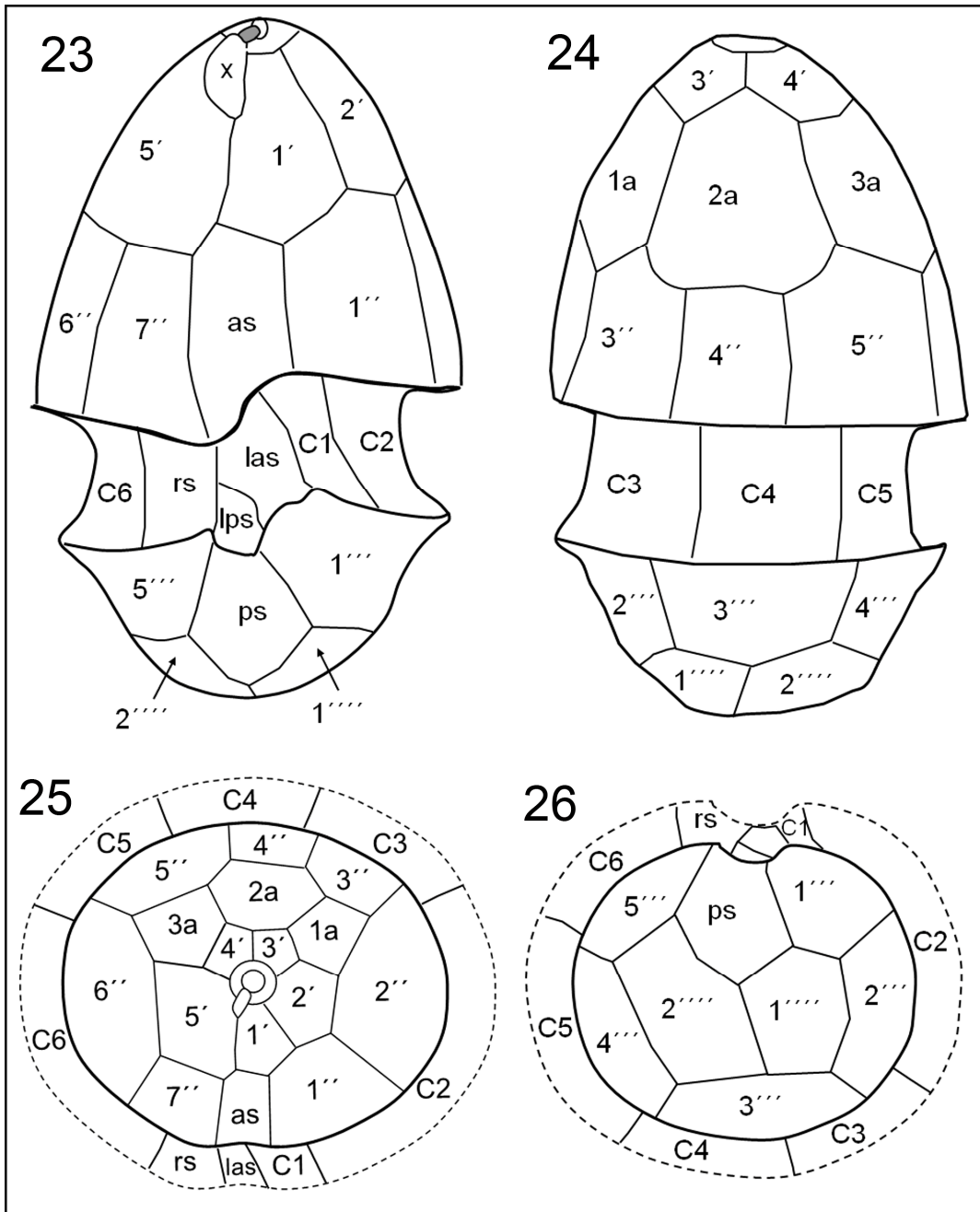
^a results on mature scales



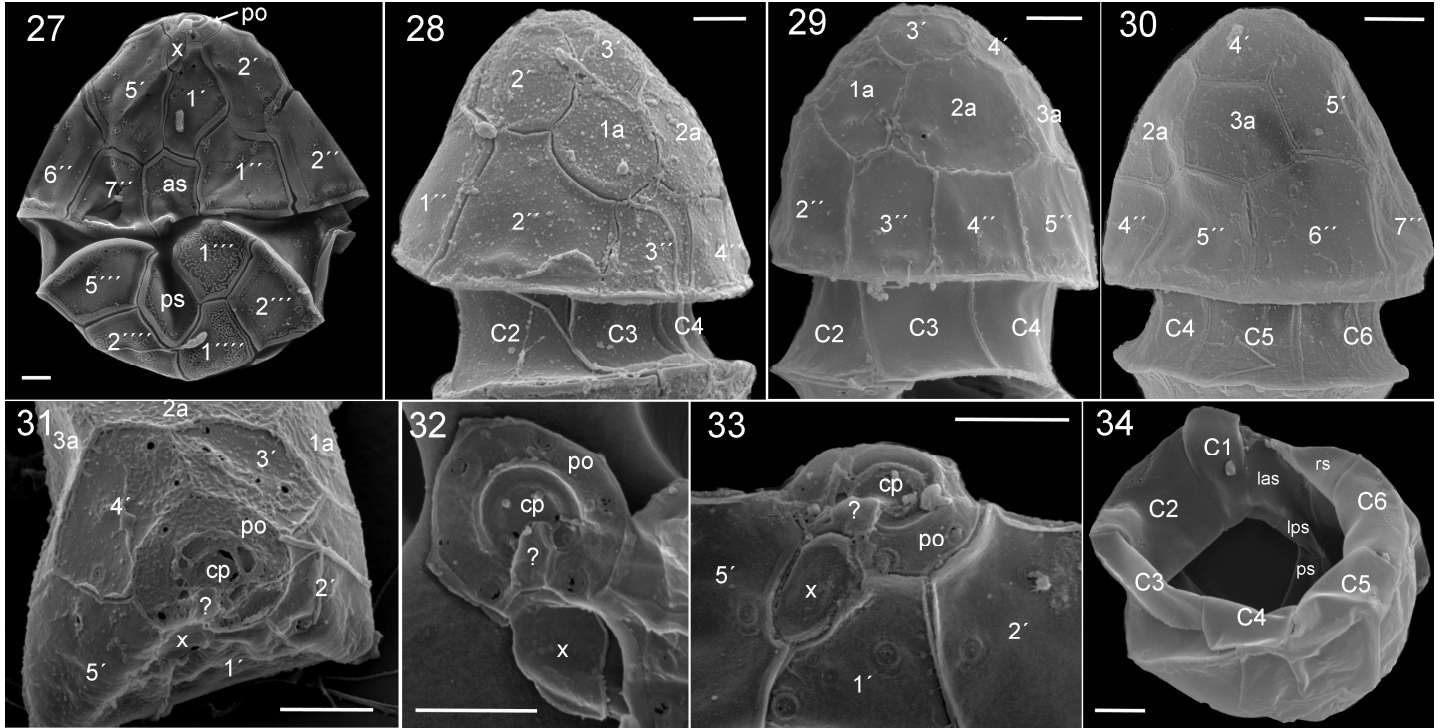
Figs 1–18. *Heterocapsa minima*. Light microscopy images of strain JK2. **Figs 1–3.** Live cells. Arrow in Fig.3 = pyrenoid. **Fig. 4.** Lugol’s-preserved cell; note the dark-stained pyrenoid. **Figs 5–6.** Same formalin-fixed cell in brightfield (Fig. 5) and with UV excitation after Calcofluor-staining (Fig. 6), showing the pyrenoid position in the cell’s left side. **Figs 7–8.** Two different focal planes of the same live cell illustrating the reticulate structure of the parietal chloroplast. **Figs 9–12.** Pairs of images showing the same formalin-fixed and DAPI stained cell in brightfield (Figs 9, 11) or with UV excitation (Figs 10, 12), showing nucleus and chloroplast shape and position. **Figs 13–14.** Two different formalin-fixed cells with UV excitation after DAPI staining. Note the nucleolus (arrow) visible in (Fig. 13). **Fig. 15.** Formalin-fixed cell showing the presence of a small red accumulation body. **Fig. 16.** Formalin-fixed cell in cell division. **Figs 17–18.** Two different formalin-fixed cells with UV excitation after calcofluor staining showing a ventral (Fig. 17) and dorsal (Fig. 18) view of the thecal plates. Scale bars: 2 μ m.



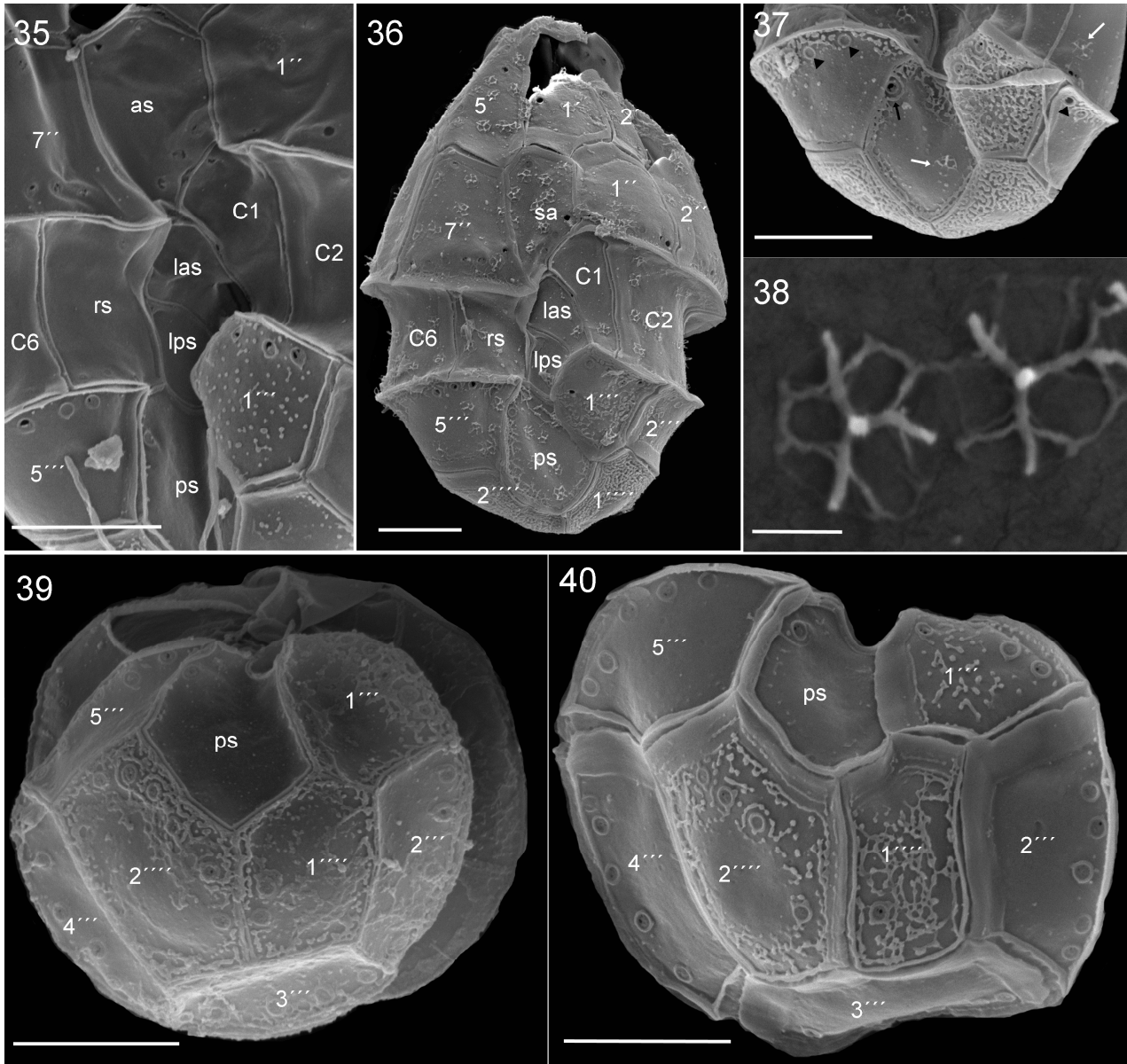
Figs. 19–22. *Heterocapsa minima*, SEM images of cells of strain JK2. **Fig. 19.** Whole cell in ventral view. **Fig. 20.** Whole cell in dorsal view. **Figs. 21–22.** Different cells likely representing normal cell shape and size (Fig. 21) and a shrunken and collapsed cell (Fig. 22). White lines indicate cell size measurement as described in the text. Scale bars = 2 μm.



Figs 23-26. *Heterocapsa minima*. Diagrammatic illustration of thecal plates. Plate labels according to the Kofoidian system. Abbreviation of sulcal plates: as=anterior sulcal; las=left anterior sulcal; lps=left posterior sulcal; rs=right sulcal; ps=posterior sulcal. **Fig. 23.** Ventral view. **Fig. 24.** Dorsal view. **Fig. 25.** Apical view. **Fig. 26.** Antapical view.



Figs 27–34. *Heterocapsa minima*. SEM micrographs of different cells. Plate labels according to the Kofoidian system. ? = plate-like structure connecting X-plate and cover plate (cp). **Fig. 27.** Whole cell in ventral view. **Fig. 28.** Epitheca in left-lateral view. **Fig. 29.** Epitheca in dorsal view. **Fig. 30.** Epitheca in right-lateral view. **Fig. 31.** Apical view showing apical plates and Apical Pore Complex (APC). **Fig. 32.** Details of the APC, Po shows six equidistant pores, cp and x plates connect through a hinge structure (marked as ?). **Fig. 33.** Detailed ventral view of APC. **Fig. 34.** Apical view of a hypotheca showing cingular and sulcal plates from inside the cell. Scale bars: 1 μm.



Figs 35–40.

Heterocapsa minima. SEM micrographs of different cells showing details of sulcal area and hypothecal plates.

Fig. 35. Detailed view of the sulcal area. as: anterior sulcal; las: left anterior sulcal; lps: left posterior sulcal; rs:

right sulcal; ps: posterior sulcal. **Fig. 36.** Cell in ventral view clearly showing sulcal plate arrangement. Note a

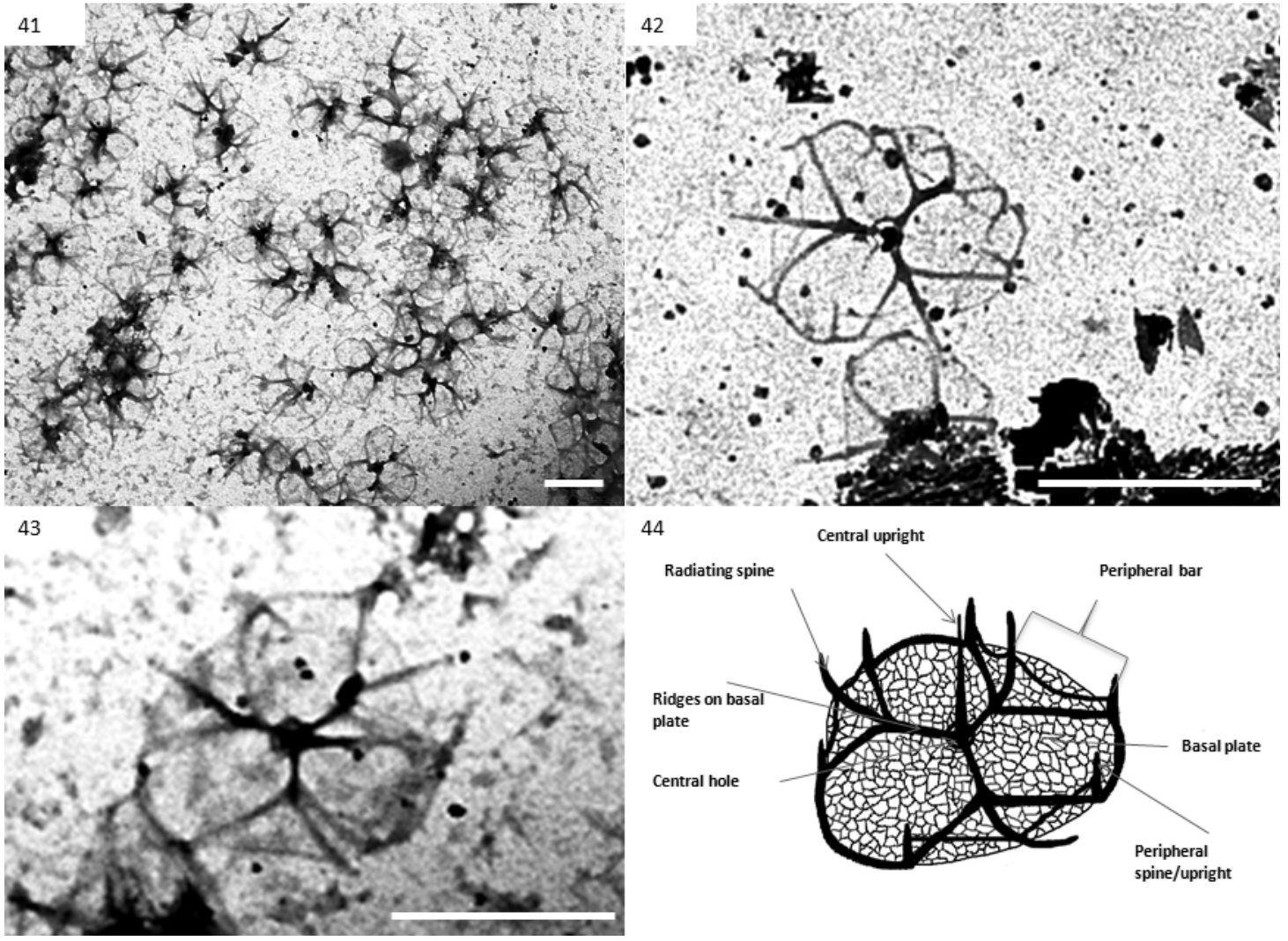
large number of body scales attached to the plates. **Fig. 37.** Dorsal view of hypotheca showing thecal pores

arranged in rows along the cingulum (arrowheads) and a pore on the posterior sulcal plate (black arrow). Note

the ornamentation of plates and attached body scales (white arrow) **Fig. 38.** Body scale detail in SEM. **Figs 39-**

40. Antapical view showing all hypothecal plates; note the plate ornamentation and the position of thecal pores.

Scale bars: 2 μm , except Fig. 38 (scales) = 0.2 μm .



Figs 41-44. TEM images of whole mount preparations of *Heterocapsa minima* (strain JK2) body scales. **Fig. 41.** Body scales of *Heterocapsa minima*. **Figs 42–43.** Detail of body scales. **Fig. 44.** Schematic line drawing of body scale showing taxonomic characters. Scale bar = 400 nm (n = 30).

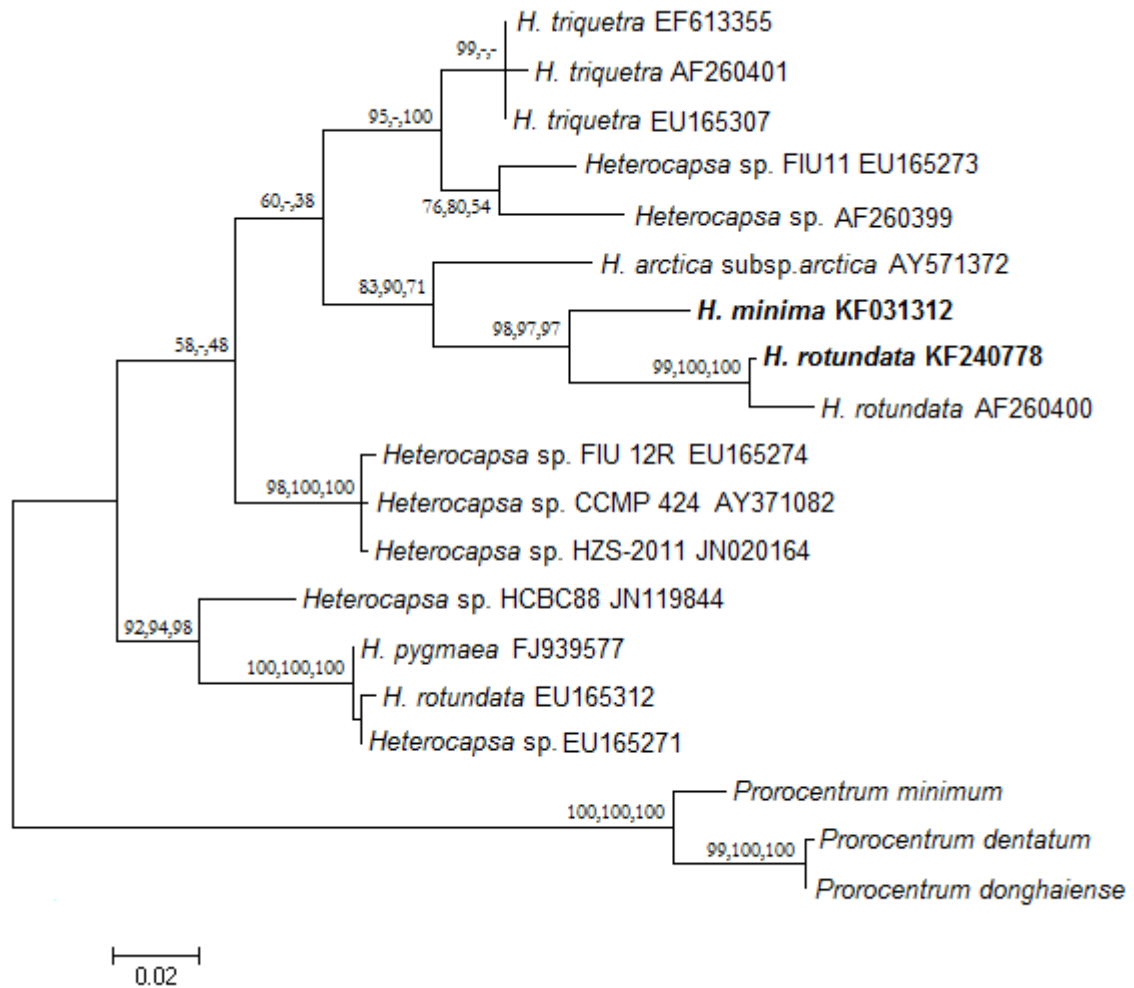


Fig. 45. Phylogenetic tree based on maximum likelihood analysis of LSU rDNA sequences from *Heterocapsa* species. *Prorocentrum minimum*, *P. dentatum* and *P. donghaiense* were used as outgroup sequences. Bootstrap values (1000 replicates) > 50 % are shown at internal nodes for maximum likelihood, maximum parsimony, and neighbour-joining analyses.

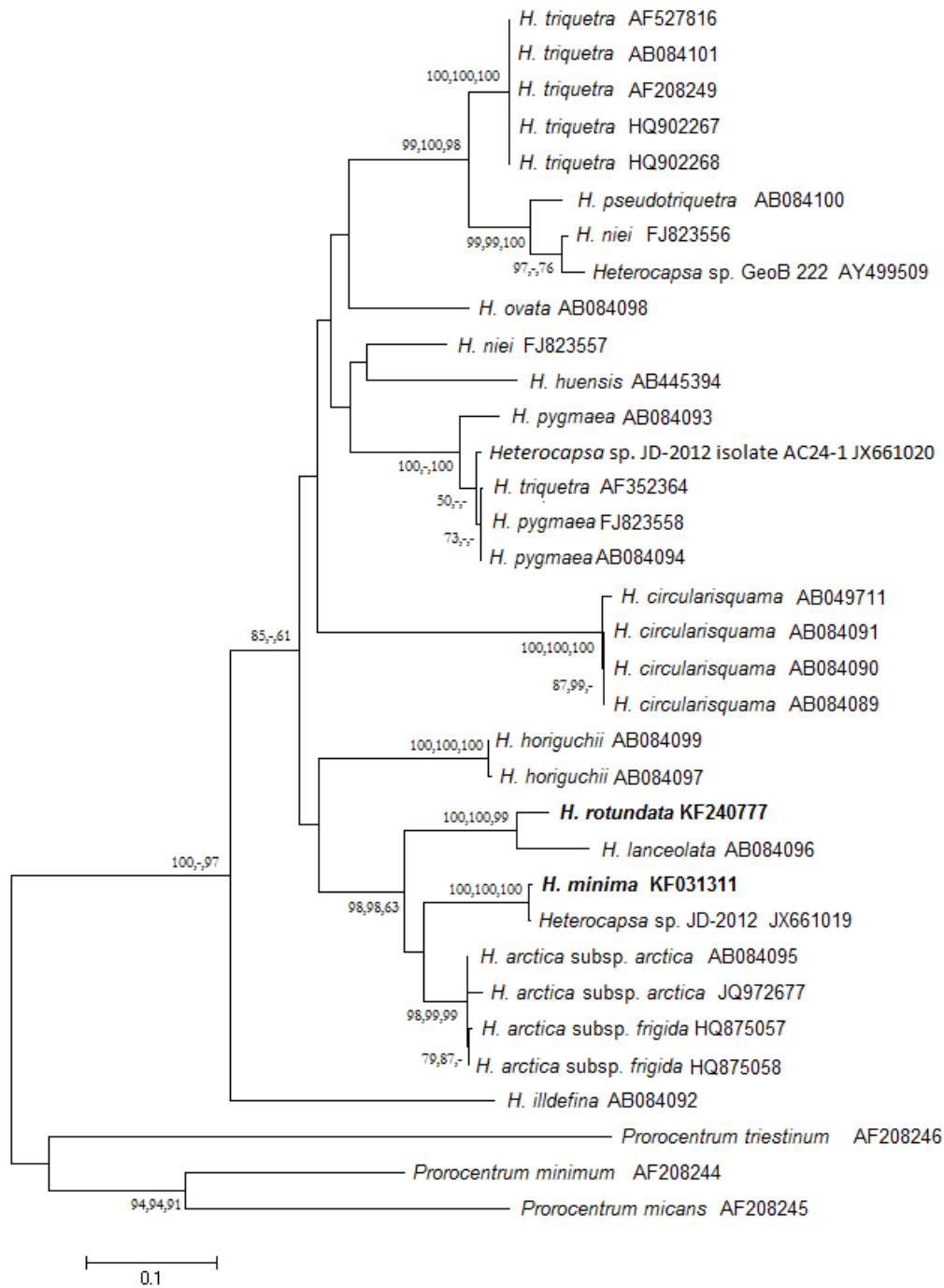


Fig. 46. Phylogenetic tree based on maximum likelihood analysis of ITS sequences from *Heterocapsa* species. *Prorocentrum minimum*, *P. triestinum* and *P. micans* were used as outgroup sequences. Bootstrap values (1000 replicates) > 50 % are shown at internal nodes for maximum likelihood, maximum parsimony, and neighbour-joining analyses.

